

**Experimental parasite infection causes genome-wide changes in DNA methylation**

Journal:	<i>Molecular Biology and Evolution</i>
Manuscript ID	MBE-19-0235.R2
Manuscript Type:	Article
Date Submitted by the Author:	n/a
Complete List of Authors:	Sagonas, Kostas; Queen Mary University of London, School of Biological and Chemical Sciences Meyer, Britta; GEOMAR, Evolutionary Ecology of Marine Fishes; Max Planck Institute for Evolutionary Biology, Max Planck Research Group Behavioural Genomics Kaufmann, Joshka; University College Cork, School of Biological, Earth & Environmental Sciences; Max Planck Institute for Evolutionary Biology, Emmy Noether Group Evolutionary Immunogenomics Lenz, Tobias; Max Planck Institute for Evolutionary Biology, Emmy Noether Group Evolutionary Immunogenomics Häslér, Robert; Kiel University, Institute of Clinical Molecular Biology Eizaguirre, Christophe; Queen Mary University of London, School of Biological and Chemical Sciences
Key Words:	DNA methylation, epigenetics, host-parasite interactions, reduced representation bisulphite sequencing, three-spined stickleback

SCHOLARONE™  
 Manuscripts

## Article - Discoveries

**Experimental parasite infection causes genome-wide changes in DNA methylation**

Kostas Sagonas<sup>1\*</sup>, Britta S. Meyer<sup>2,#</sup>, Joshka Kaufmann<sup>3,4</sup>, Tobias L. Lenz<sup>4</sup>, Robert Häsler<sup>5</sup>,  
Christophe Eizaguirre<sup>1</sup>

<sup>1</sup>School of Biological and Chemical Sciences, Queen Mary University of London, London, UK

<sup>2</sup>Evolutionary Ecology of Marine Fishes, GEOMAR Helmholtz Centre for Ocean Research, Kiel,  
Germany

<sup>3</sup>School of Biological, Earth & Environmental Sciences, University College Cork, Cork, Republic  
of Ireland

<sup>4</sup>Research Group for Evolutionary Immunogenomics, Max Planck Institute for Evolutionary  
Biology, Plön, Germany

<sup>5</sup>Institute of Clinical Molecular Biology, Kiel University, Kiel, Germany

# present address: Max Planck Research Group Behavioural Genomics, Max Planck Institute for  
Evolutionary Biology, Plön, Germany

\* Corresponding Author: Kostas Sagonas, email: [k.sagonas@qmul.ac.uk](mailto:k.sagonas@qmul.ac.uk)

## 21 Abstract

22 Parasites are arguably among the strongest drivers of natural selection, constraining hosts to evolve  
23 resistance and tolerance mechanisms. Although, the genetic basis of adaptation to parasite  
24 infection has been widely studied, little is known about how epigenetic changes contribute to  
25 parasite resistance and eventually, adaptation. Here, we investigated the role of host DNA  
26 methylation modifications to respond to parasite infections. In a controlled infection experiment,  
27 we used the three-spined stickleback fish, a model species for host-parasite studies, and their  
28 nematode parasite *Camallanus lacustris*. We showed that the levels of DNA methylation are  
29 higher in infected fish. Results furthermore suggest correlations between DNA methylation and  
30 shifts in key fitness and immune traits between infected and control fish, including respiratory  
31 burst and functional trans-generational traits such as the concentration of motile sperm. We  
32 revealed that genes associated with metabolic, developmental and regulatory processes (cell death  
33 and apoptosis) were differentially methylated between infected and control fish. Interestingly,  
34 genes such as the *neuropeptide FF receptor 2* and the *integrin alpha 1* as well as molecular  
35 pathways including the Th1 and Th2 cell differentiation were hypermethylated in infected fish,  
36 suggesting parasite-mediated repression mechanisms of immune responses. Altogether, we  
37 demonstrate that parasite infection contributes to genome-wide DNA methylation modifications.  
38 Our study brings novel insights into the evolution of vertebrate immunity and suggests that  
39 epigenetic mechanisms are complementary to genetic responses against parasite-mediated  
40 selection.

41  
42 **Keywords:** DNA methylation, epigenetics, host-parasite interactions, reduced representation  
43 bisulfite sequencing, three-spined stickleback

44

## 45 **Introduction**

46 Evolutionary theory predicts that the adaptive potential of a population primarily relies on its  
47 genomic variation (Frankham et al. 2002). In the case of rapid environmental changes, individuals  
48 are unlikely to be pre-adapted to survive under the new conditions and, as such, phenotypic  
49 plasticity may play a central role in population rescue (Merilä and Hendry 2014). Phenotypic  
50 plasticity refers to the capacity of a genotype to produce different phenotypes under different  
51 environmental conditions and is mostly modulated by the regulation of gene expression (West-  
52 Eberhard 2003). Resolving the molecular basis of phenotypic plasticity could hence be the missing  
53 piece of the puzzle for a better understanding of the adaptive potential of populations or species  
54 (Eizaguirre and Baltazar-Soares 2014; Rey et al. 2019).

55 Epigenetic mechanisms are important environment-modulated mechanisms possibly  
56 accelerating adaptive responses to selection (Gugger et al. 2016; Artemov et al. 2017; Metzger and  
57 Schulte 2017). Although several epigenetic pathways can facilitate phenotypic plasticity (e.g.,  
58 histone modifications, chromatin remodeling, small interfering RNAs), the addition of a methyl  
59 group to cytosine nucleotides is probably the best characterized to date (Skvortsova et al. 2018).  
60 While there exists DNA methylation resetting mechanisms in the early embryo (Potok et al. 2013;  
61 Seisenberger et al. 2013), recent evidence suggests that reprogramming may be incomplete and  
62 acquired DNA methylation states may be transmitted from parents to offspring (Metzger and  
63 Schulte 2017). This offers an alternative mode of inheritance, which could influence evolutionary  
64 trajectories of populations (Smith et al. 2016; Kronholm et al. 2017; Rey et al. 2019).

65 Multiple studies on natural populations have found links between variation in DNA  
66 methylation and ambient abiotic factors such as temperature (Gugger et al. 2016), salinity  
67 (Artemov et al. 2017) and even oil spill pollution (Robertson et al. 2017). In nature, inter-species  
68 interactions also affect populations' evolution. Among these interactions, parasites are one of the  
69 most potent selective pressures affecting the genetic diversity of host populations (Béréanos et al.  
70 2011; Eizaguirre et al. 2012), modifying species composition (Altizer et al. 2003), altering gene  
71 expression of their host (Lenz et al. 2013) and even changing the selection environment of  
72 subsequent host generations (Brunner et al. 2017). Parasites, however, constantly evolve and their  
73 communities change within and between seasons. Therefore, in order to counter parasite-induced  
74 fitness costs, hosts responses must include plastic and effective components (Brunner and  
75 Eizaguirre 2016).

1  
2  
3 76 Even though genetic components are important for a rapid inter-generational response to  
4  
5 77 parasite selection (Eizaguirre et al. 2012), previous reports have shown that responses might also  
6  
7 78 be independent of the host's genetic background, suggesting alternative non-genetic mechanisms  
8  
9 79 facilitating host-parasite interactions (Kaufmann et al. 2014; Beemelmans and Roth 2017). While  
10  
11 80 much of the epigenetic makeup, including DNA methylation, is determined during cellular  
12  
13 81 differentiation and development, parasites may induce changes in the DNA methylation profile of  
14  
15 82 mature immune cells that can alter the accessibility of transcription factors to genes (Morandini et  
16  
17 83 al. 2016). In this way, DNA methylation can immediately influence hosts' resistance and tolerance  
18  
19 84 to parasites, with likely consequences for the evolution of host-parasite interactions. Ultimately,  
20  
21 85 inheritance of DNA methylation modifications induced by parasite infection may provide  
22  
23 86 resistance to the next host generation. This is particularly evolutionary relevant since offspring are  
24  
25 87 likely to experience a similar pathogenic selective environment as their parents.

24 88 Although, interesting insights regarding the effects of DNA methylation to plasticity and  
25  
26 89 adaptation come from exploring natural populations (Liu et al. 2015; Smith et al. 2015; Gugger et  
27  
28 90 al. 2016; Thorson et al. 2017), there has so far been limited effort on vertebrates to combine  
29  
30 91 ecological experimental approaches with DNA methylation (Artemov et al. 2017; Metzger and  
31  
32 92 Schulte 2017; Heckwolf et al. 2019). DNA methylation is associated with the nucleotide sequence  
33  
34 93 itself (Dubin et al. 2015), influenced by the environmental heterogeneity (Sheldon et al. 2018) and  
35  
36 94 is altered by methyltransferase errors that generate spontaneous stochastic DNA methylation  
37  
38 95 modifications (Riggs et al. 2007). Therefore, controlled experiments are required to establish the  
39  
40 96 functional link between DNA methylation changes and their physiological consequences (e.g.,  
41  
42 97 Heckwolf et al. 2019). To investigate how parasites change the DNA methylation profile of their  
43  
44 98 hosts and whether these modifications are associated with parasite resistance and tolerance, we  
45  
46 99 conducted a controlled laboratory split-clutch infection experiment using the three-spined  
47  
48 100 stickleback (*Gasterosteus aculeatus*) model system. This fish is an ideal vertebrate organism for  
49  
50 101 studying responses to parasite infection, since it exhibits a well-documented parasite fauna  
51  
52 102 (Eizaguirre et al. 2012; Kaufmann et al. 2014). In a recent split-clutch design experiment,  
53  
54 103 Kaufmann and colleagues (2014) demonstrated transgenerational effects of parasite resistance to  
55  
56 104 the nematode *Camallanus lacustris*, a common parasite, with clear fitness benefits for the  
57  
58 105 offspring, but the underlying mechanisms awaited investigation. Based on this previous study,  
59  
60 106 using Reduced Representation Bisulfite Sequencing (RRBS) (Meissner et al. 2005), we focused

1  
2  
3 107 on the methylation of cytosine-phosphate-guanine dinucleotides (CpG sites), the most common  
4  
5 108 methylation motif in vertebrates. We investigated whether parasite infection alters genome-wide  
6  
7 109 patterns of DNA methylation and numbers of methylated sites. We also tested if fitness traits  
8  
9 110 correlate with changes in DNA methylation and if parasite-induced DNA methylation  
10  
11 111 modifications are associated with specific gene functions.  
12

## 13 113 **Results**

### 14 114 **Effect of parasite infection on fish phenotypes**

15 115 We performed a split-clutch design. After laboratory breeding of wild-caught fish, we randomly  
16  
17 116 assigned parasite-free juvenile brothers of five fish families ( $N \geq 10$  per family; supplementary  
18  
19 117 table S1, Supporting Information Appendix I) to one of two treatment groups: no parasite exposure  
20  
21 118 (i.e., control) or exposed with *C. lacustris*, in order to control for the family genetic background,  
22  
23 119 and tested the effects of parasite infection on fish fitness. We measured fitness traits (e.g., the  
24  
25 120 weight of liver, head kidney and testis, motile sperm concentration) for a total of 52 males (i.e., 25  
26  
27 121 infected and 27 uninfected fish). To control for dosage-effect, we exposed each fish twice to  
28  
29 122 exactly six larvae of *C. lacustris*. All experimental procedures of controlled fish infection via  
30  
31 123 ingestion of infected copepods are described in Eizaguirre et al. (2012) and Kaufmann et al. (2014).  
32  
33 124 We verified that all exposed fish were infected by the parasites by dissecting them (Kaufmann et  
34  
35 125 al. 2014). Parasite infection had significant impact on fish condition-dependent traits, with infected  
36  
37 126 fish having smaller head kidney ( $F_{1,42} = 9.11$ ,  $P = 0.004$ ) and liver ( $F_{1,42} = 5.06$ ,  $P = 0.029$ ), after  
38  
39 127 correcting for body size, compared to control fish. Furthermore, we found that infected fish were  
40  
41 128 less heavy than uninfected ones ( $767.29 \pm 294.62$  mg vs  $848.11 \pm 228.43$  mg;  $F_{1,44} = 5.41$ ,  $P =$   
42  
43 129  $0.024$ ), although the mean fish length showed no significant differences ( $40.25 \pm 4.47$  mm vs  $41.15$   
44  
45 130  $\pm 3.58$  mm;  $F_{1,44} = 2.52$ ,  $P = 0.119$ ). Consequently, the body condition of infected fish was lower  
46  
47 131 than that of control fish ( $-0.03 \pm 0.1$  vs  $0.03 \pm 0.09$  respectively;  $F_{1,46} = 4.42$ ,  $P = 0.041$ ). The  
48  
49 132 comparison of the weight of testes (corrected for fish length,  $F_{1,41} = 0.05$ ,  $P = 0.831$ ) and motile  
50  
51 133 sperm concentration ( $F_{1,12} = 1.74$ ,  $P = 0.211$ ) showed no differences between infected and control  
52  
53 134 fish. Overall, these results show significant costs of parasite infection in stickleback fish and  
54  
55 135 characterize the need for hosts to evolve plastic responses (for more details about costs of  
56  
57 136 parasitism in this experiment, see Kaufmann et al. (2014)).  
58  
59 137

### 138 **Parasite infection induces changes in numbers of DNA methylated sites**

139 Liver tissues were isolated immediately upon fish dissections, preserved in RNAlater at  $-20^{\circ}\text{C}$  and  
140 DNA methylation was screened using RRBS (Meissner et al. 2005; Heckwolf et al. 2019) for 52  
141 fish (25 infected vs 27 uninfected males). For each fish, a single-end library of 100 bp with an  
142 average size of 11.5 million reads was produced. Library preparation was carried out at the Institute  
143 for Clinical Molecular Biology (IKMB; Germany) and sequencing was conducted on an Illumina  
144 HiSeq 2500 platform. To control for sequence bias due to the positive correlation between the  
145 number of CpG sites and the number of reads sequenced ( $t = 10.01$ ,  $df = 48$ ,  $P < 0.001$ ), we  
146 estimated the ratio of methylated sites (RMS) and the ratio of methylated regions (RMR; defined  
147 as genomic regions and identified as a sliding window size of 100 bases and step size of 100 bases),  
148 dividing the number of methylated CpG sites/regions by the number of reads. Fish exposed to *C.*  
149 *lacustris* had higher ratio of DNA methylated sites (RMS:  $0.063 \pm 0.006$  vs  $0.059 \pm 0.006$ ;  $t =$   
150  $2.13$ ,  $df = 47.16$ ,  $P = 0.038$ ) than control fish. Because of genetic effects linked to family  
151 background, we repeated the former analysis using family as random effect. Likewise, linear  
152 mixed effect models (LMM) showed that RMS were different between groups, with infected fish  
153 having substantially more CpG methylated sites than their uninfected counterparts ( $F_{1,44} = 4.97$ ,  $P$   
154  $= 0.031$ ), though no differences were observed in the overall fractional methylation (fig. 1 and  
155 supplementary table S2, SI Appendix I). The increase in methylated CpGs was proportionally  
156 random across the different genomic features, i.e. promoters, exons, introns and intergenic regions  
157 (chi-square test;  $\chi^2 = 0.023$ ,  $P = 0.999$ ; SI Appendix I Figure S1). In contrast, RMR showed no  
158 difference between treatments (RMR:  $F_{1,44} = 1.48$ ,  $P = 0.230$ , supplementary table S2,  
159 Supplementary Appendix I).

160 We converted the methylation frequency into a diploid genotype (hereafter, Single  
161 Methylation Polymorphism; SMPs) to estimate the Wright's fixation index ( $F_{\text{ST}}$  and  $F_{\text{IS}}$ ; we will  
162 refer to the DNA methylation  $F_{\text{ST}}$  as epi- $F_{\text{ST}}$ , and epi- $F_{\text{IS}}$  respectively) between infected and  
163 control fish. To do so, non-methylated sites (methylation frequency;  $MFr < 30\%$ ) were annotated  
164 as 0/0, heterozygote methylated sites ( $30\% < MFr < 70\%$ ) were converted into 0/1, whereas  
165 homozygote methylated sites ( $MFr > 70\%$ ) annotated as 1/1. We found that infected fish displayed  
166 lower epi- $F_{\text{ST}}$  (epi- $F_{\text{ST}}$  test:  $F_{1,560} = 20.24$ ,  $P < 0.001$ ) and higher epi- $F_{\text{IS}}$  values (-0.28 vs. -0.32).  
167 Together, the lower differentiation in methylation pattern of infected fish compared to their

1  
2  
3 168 conspecific control, suggests homogenization of the methylome upon infection, independently of  
4  
5 169 the family background similar to what happens for gene expression (Lenz et al. 2013).  
6  
7 170

### 8 171 **DNA methylation profile across individuals**

9  
10 172 In order to better characterize changes on the methylome in response to parasite infection, we  
11  
12 173 investigated the distribution of methylated CpG sites/regions across individual fish. From the CpG  
13  
14 174 sites/regions sequenced, we retained those that were observed in at least two individual fish and  
15  
16 175 had a coverage higher than 10X. We found that methylated CpGs were similarly distributed across  
17  
18 176 genomic features between control (promoter: 18.61%; exon: 14.44%; intron: 23.71%; intergenic:  
19  
20 177 43.24%) and infected (promoter: 19.09%; exon: 15.03%; intron: 23.22%; intergenic: 42.66%) fish  
21  
22 178 ( $\chi^2 = 0.06$ ,  $P = 0.996$ ; SI Appendix I Figure S1). Using the fractional methylation data, calculated  
23  
24 179 as the number of methylated cytosines over the number of cytosines per site, we performed cluster  
25  
26 180 analyses considering all methylated CpGs. Our findings showed that fish group following their  
27  
28 181 family genetic background (Fig. 2). In particular, goodness of fit for non-metric dimensional  
29  
30 182 scaling (NMDS) plot suggested the presence of five dimensions with a stress value lower than 0.1  
31  
32 183 that also fits the number of fish families sequenced. Similarly,  $k$ -mean and hierarchical clustering  
33  
34 184 suggested the presence of three major clusters and a family- rather than treatment- specific  
35  
36 185 clustering (fig. 2C and SI Appendix I Figure S2). When differentially methylated regions were  
37  
38 186 used (SI Appendix II), similar results were observed, with families being well distinguished from  
39  
40 187 one another (SI Appendix II Figure S1).

41  
42 188 Pairwise genetic  $F_{ST}$  values were lower within (in all cases lower than 0.001) than between  
43  
44 189 (ranged from 0.099 to 0.199) families (supplementary table S3, SI Appendix I). Conversely,  
45  
46 190 principal component analysis (PCA) showed a less structured clustering of families, with the first  
47  
48 191 two principal components explaining jointly 11.8% of the methylome variation (fig. 2B). Overall,  
49  
50 192 our result show that fish methylomes cluster by family background. Such a result is to be expected  
51  
52 193 since the probability of CpG sites to be methylated depends on the underlying genetic code which  
53  
54 194 varies among families.  
55  
56 195

### 51 196 **Differential methylation between treatments**

53 197 We then focused on those specific CpG sites and regions which were differentially methylated  
54  
55 198 between treatment groups. We found a total of 1,973 CpG sites out of 1,172,887 CpGs (0.17%)  
56  
57  
58  
59  
60



1  
2  
3 199 across the genome that showed at least 15% differential fractional methylation (DMS;  $q < 0.01$ )  
4 200 between infected and uninfected fish (fig. 3). Those positions were located in 314 differentially  
5 201 methylated regions (DMR). Infected fish had more hypermethylated sites (1164 vs 810; Fisher  
6 202 test;  $\chi^2 = 6.48$ ,  $P = 0.016$ ) and regions (194 vs 120; Fisher test;  $\chi^2 = 11.52$ ,  $P = 0.001$ ) than  
7 203 uninfected fish (fig. 3 and supplementary table S2, SI Appendix I). The differentially methylated  
8 204 sites and regions were predominately found in intergenic regions (47.74% and 48.94%,  
9 205 respectively), with introns (26.19% and 23.09), exons (15.07% and 13.98%) and promoters (11%  
10 206 and 13.98%) showing lower proportions (see also SI Appendix I Figure S1 and SI Appendix II for  
11 207 more details).

12 208 Cluster analyses for the fractional methylation data such as  $k$ -mean statistics and goodness  
13 209 of fit for differentially methylated sites (DMSs; fig. 4) and regions (DMRs; SI Appendix II Figure  
14 210 S2) indicated the presence of two groups that match the infection treatments (infected or control;  
15 211 Shimodaira-Hasegawa test between the observed clustering and a treatment specific clustering for  
16 212 DMSs:  $P = 0.501$  and for DMRs:  $P = 0.487$ ). A PCA showed that the first two principal  
17 213 components explained 38.4% of the variation in differentially methylated sites, and the two  
18 214 treatments were separated along PC2 (15.5% of the variance, fig. 4A). PC1 indicated genetic  
19 215 background and to a lesser extent treatment as a predictor, where families with lower pairwise  $F_{ST}$   
20 216 values (supplementary table S3, SI Appendix I) grouped together. Our results hence show that  
21 217 differential methylation of specific CpG positions is linked both to infection as well as the  
22 218 underlying available genetic background for methylation.

23  
24  
25  
26  
27  
28  
29  
30  
31  
32  
33  
34  
35  
36  
37  
38  
39

## 220 **Functional annotation and pathways analysis between treatments**

40 221 Using the available reference genome, functional enrichment and pathway analyses were carried  
41 222 out to identify functional associations among genes that were differentially methylated upon  
42 223 parasite challenge. Differentially methylated sites were associated with 132 unique genes (80  
43 224 genes were hypermethylated for infected fish and 52 for uninfected fish; supplementary table S4,  
44 225 SI Appendix I). At a false discovery rate threshold of 0.05, gene category enrichment analysis  
45 226 revealed that infected and uninfected fish had significant differences in 34 biological process (BP),  
46 227 9 cellular component (CC) and 23 molecular function (MF) GO terms. Significant BP, CC and MF  
47 228 GO terms included several biosynthetic and metabolic processes, signaling pathways and  
48 229 regulation of cell migration (fig. 5 and supplementary table S5, SI Appendix I). A number of genes  
49  
50  
51  
52  
53  
54  
55  
56  
57  
58  
59

1  
2  
3 230 with differential methylation signal (thereafter referred to as differentially methylated genes) are  
4  
5 231 involved in the regulation of transcription and transfer of methyl-groups (e.g., *sp5l*, *elmsan1b*,  
6  
7 232 *polr3b*, *mepce*), in the regulation of immune response and inflammation activity (e.g., *colec12*,  
8  
9 233 *fbxo41*, *march7*, *itga1* and *npffr2b*), and in the regulation of cell cycle and apoptosis (e.g., *blcap*,  
10  
11 234 *stambpb* and *rgcc*). Interestingly, several genes that are directly or indirectly associated with the  
12  
13 235 regulation of immune response (e.g. *prg4*, *fbxo41*, *colec12* and *march7*) and transcription (e.g.  
14  
15 236 *polr3b*, *mepce*, *sp5l* and *elmsan1b*) were significantly hypomethylated in infected fish compared  
16  
17 237 to control. A complete report of every sequence including full gene ontology terms is presented in  
18  
19 238 supplementary table S4 (SI Appendix I).

20  
21 239 Kyoto Encyclopedia of Genes and Genomes (KEGG) enrichment analysis identified a  
22  
23 240 number of molecular pathways associated with hypermethylated genes after *C. lacustris* infection.  
24  
25 241 The top pathways were purine metabolism and the biosynthesis of antibiotics that are both  
26  
27 242 associated with immune responses (e.g., Seegmiller et al. 1977; Li and Gatlin 2006). Furthermore,  
28  
29 243 we detected a number of other metabolic or immune pathways such as the Th1 and Th2 cell  
30  
31 244 differentiation and the T-cell receptor signaling pathway (supplementary table S6, SI Appendix I).

32  
33 245 Analogous to DMS, DMR revealed a similar pattern and a number of identical genes and  
34  
35 246 pathways associated to immune responses (e.g. *npffr2b*, the purine metabolism pathway),  
36  
37 247 metabolism (e.g. *prss1*, *tdh*) and development (e.g. *pde1a*, *cryba2b*) separated treatment groups.  
38  
39 248 The detailed findings from DMR analyses that support the results of DMS are provided in  
40  
41 249 Supplementary Information Appendix II.

42  
43 250 To test whether the differences detected between treatment groups are real and robust and to  
44  
45 251 evaluate parasite-induced DNA methylation modifications and their association with genes  
46  
47 252 involved in immunity regulation, we performed a randomization test. Specifically, treatment  
48  
49 253 assignment (exposed versus not-exposed) was randomized 100 times and the output was compared  
50  
51 254 to the original data. To produce genetically balanced random permutations similar to the original  
52  
53 255 dataset, treatment assignment was randomized within families. Differential methylation and  
54  
55 256 functional annotation analyses in the randomized sets revealed several DMS and associated  
56  
57 257 transcripts, respectively. However, their numbers were on average two times lower than the  
58  
59 258 original dataset (fig. 3C). Importantly, in all independent runs, several transcripts were consistently  
60  
61 259 identified, and the vast majority of transcripts were linked to developmental processes,  
62  
63 260 biosynthesis or other cellular processes and no or few correlated with immunity and importantly

1  
2  
3 261 did not capture genes found in the original dataset (*prg4* and *itga1*) (see also SI Appendix I Figure  
4  
5 262 S3). This suggests a base line structure due to differential treatments. Overall, these findings  
6  
7 263 reinforce the view that the differences detected and the links to parasite resistance and immunity  
8  
9 264 in the original dataset are biologically relevant and not the results of unnoticed experimental  
10  
11 265 artifact.

12 266

### 13 267 **DNA methylation modifications and fish fitness**

14  
15 268 To clarify whether modifications in DNA methylation are part of an adaptive response to parasite  
16  
17 269 infection, we correlated the ratio of methylated sites with fitness traits. RMSs were selected  
18  
19 270 because they represent a good index of the overall hyper- or hypo- methylation of the DNA. Our  
20  
21 271 findings showed significant interactions between treatment and i) respiratory burst activity  
22  
23 272 (measure of innate immune response;  $F_{2,39} = 4.57$ ,  $P = 0.039$ ), ii) liver weight ( $F_{2,40} = 5.26$ ,  $P =$   
24  
25 273  $0.009$ ), iii) head kidney weight ( $F_{2,40} = 4.29$ ,  $P = 0.021$ ) and iv) motile sperm concentration ( $F_{1,10}$   
26  
27 274  $= 10.50$ ,  $P = 0.009$ ) on RMS. However, body condition ( $F_{2,40} = 2.09$ ,  $P = 0.137$ ) or testes weight  
28  
29 275 ( $F_{2,39} = 0.74$ ,  $P = 0.485$ ) showed no significant association with RMS (SI Appendix I Figure S4).  
30  
31 276 Furthermore, for each infected fish we estimated the deviation of its DNA methylation pattern  
32  
33 277 from the control group as the mean Euclidean distance of the given fish from control fish and  
34  
35 278 correlated it to its mean difference in body condition compared to the control group. The  
36  
37 279 comparison showed a negative correlation between mean epi- $F_{ST}$  and body condition shifts ( $t = -$   
38  
39 280  $2.175$ ,  $df = 20$ ,  $r = -0.44$ ,  $P = 0.042$ ), whereby infected fish that modified their methylomes more  
40  
41 281 extensively showed a level of body condition closer to that of control fish.

42  
43 282 In addition, in the exposed group, correlation tests were carried out for significantly  
44  
45 283 hypomethylated genes related to parasite resistance to examine whether their levels of  
46  
47 284 hypomethylation are associated with increased fitness. To do so, we summarized fitness-related  
48  
49 285 traits into single fitness index obtained from a PCA. PC scores were then correlated to these genes'  
50  
51 286 methylation levels. PCA showed that PC1 and PC2 explained jointly 60.6% of fitness variation  
52  
53 287 (35.4% and 25.2%, respectively), with liver weight and respiratory burst activity contributing  
54  
55 288 68.6% of the variance in PC1, while gonads and head kidney weight explained 86.3% of PC2.  
56  
57 289 Correlation tests between PC1 or PC2 and fractional methylation in genes revealed that genes  
58  
59 290 involved in the regulation of immune response, including *fbxo41* ( $r = -0.35$ ,  $P = 0.033$ ), *march7* ( $r = -$   
60  
291  $-0.64$ ,  $P < 0.001$ ) and *tpbgb* ( $r = -0.44$ ,  $P = 0.008$ ), as well as DNA transcription (*dnaja3b*:  $r = -$

1  
2  
3 292 0.62,  $P < 0.001$ ) were negatively correlated, suggesting that lower methylation were associated  
4  
5 293 with higher fitness related traits. Overall, these results bring evidence for a potential link between  
6  
7 294 changes in fish physiology due to parasite infection and DNA methylation modifications.  
8  
9 295

## 10 296 **Discussion**

11 297 Although evidence points towards epigenetic mechanisms contributing to phenotypic plasticity to  
12 298 respond to abiotic environmental changes (Kawakatsu et al. 2016; Artemov et al. 2017), we still  
13 299 know surprisingly little about the epigenetic mechanisms involved in species-species interactions.  
14 300 Our experimental study shows that stickleback fish exposed and infected with one of their common  
15 301 nematode parasites, *C. lacustris*, had significantly more methylated sites than their non-infected  
16 302 counterparts. This did not translate however into differences in overall fractional methylation. We  
17 303 also show that DNA methylation modifications correlate with immune-related traits such as the  
18 304 respiratory burst as well as with the concentration of motile sperm – an important trans-  
19 305 generational fitness-related trait. Interestingly, we detected a pattern of differential methylation  
20 306 that reflects treatment-specific selection. These differences translated into functional enrichments  
21 307 with both over- and under-representation of GO terms involved in immune and metabolic  
22 308 processes, two physiological processes associated with parasite resistance and tolerance.

23 309 Hosts suffer a double cost of infection because parasites use them as sources of nutrients but  
24 310 also force them to induce an immune response resulting in overall fitness costs (Bize et al. 2010).  
25 311 Our study confirms such costs, as infected fish showed lower body condition and relative organ  
26 312 weights, all markers of health status and fitness (Kurtz et al. 2006; Eizaguirre et al. 2009),  
27 313 compared to uninfected fish. Controlling for genetic effects with a split clutch design, we show  
28 314 that infected fish had an overall increased ratio and hence number of CpG methylation sites as well  
29 315 as 62% more hypermethylated genomic regions than their non-infected brothers. This increase in  
30 316 mean genome-wide methylation level was negatively associated with the interaction of treatment  
31 317 and fitness related traits, including the respiratory burst activity- a known cell-mediated response  
32 318 of the innate immune pathway (SI Appendix I Figure S4). Remarkably, fish that modified their  
33 319 methylomes more extensively coped better with infection and maintain a body condition closer to  
34 320 uninfected fish. This, together with the negative correlation between the fractional methylation of  
35 321 hypomethylated genes among infected fish and their overall fitness, provides first evidence that  
36 322 methylome modifications is a part of the response to parasite infection. Methylation of specific

1  
2  
3 323 genes has also been shown to lead sticklebacks closer to control phenotypes upon salinity  
4 challenges (Heckwolf et al. 2019) Finally, DNA methylation modifications correlated with the  
5 324 interaction of treatment and motile sperm concentration, a fertility trait related to offspring body  
6 325 condition (Kekäläinen et al. 2015; Alavioon et al. 2017). Using sperm competition trials Kaufman  
7 326 et al (2014) showed that such sperm deficiencies in infected sticklebacks compared to their  
8 327 uninfected brothers functionally translated into reduced reproductive success and reduced hatching  
9 328 success and survival. Taken together, our results are consistent with previous studies (Downen et  
10 329 al. 2012; Marr et al. 2014; Hu et al. 2018) suggesting that parasite infection requires hosts to  
11 330 reshape their methylation profile with consequences on fitness-related traits and reproductive  
12 331 success. Yet, considering the complexity of physiological processes, further studies will need to  
13 332 exactly on the adaptive value and inheritance of DNA methylation on parasite resistance. Noting,  
14 333 that the presence of DMS detected and the general enrichment (yet significantly smaller than the  
15 334 original dataset) in the randomized runs is likely associated with the fact that i) fish were laboratory  
16 335 bred and maintained under standardized conditions, ii) we focused on exposed vs unexposed fish  
17 336 which results in variation in actual infection and therefore also homogenizes the groups. This is  
18 337 however the most ecologically relevant comparisons since in nature it is impossible to know  
19 338 whether an uninfected fish has been exposed to parasites or not. Furthermore, our findings suggest  
20 339 that fish are capable of adjusting their phenotypes and physiology to laboratory conditions.  
21 340

22 341 In this study, we show that infected fish displayed less differentiation in methylation pattern  
23 342 than control fish. Similarly to genome-wide transcription patterns (Lenz et al. 2013), we show that  
24 343 upon infection, methylomes of infected fish converge towards a similar response, indicating the  
25 344 activation of similar host responses. This suggests that parasite pressure is strong enough to trigger  
26 345 a response that requires co-opting of gene networks. Moreover, we found 1,973 differentially  
27 346 methylated CpG across 314 genomic regions. About 80% of these sites and regions of infected  
28 347 fish were located in intragenic and intergenic CpGs while the remaining 20% were linked to  
29 348 promoters. Although, the correlation between promoter methylation and gene expression has long  
30 349 been recognized (Bird 1984), recent findings suggests that gene body methylation can regulate  
31 350 genome-wide splicing patterns (Lev Maor et al. 2015), alter chromatin structure (Lorincz et al.  
32 351 2004), regulate alternative promoters (Maunakea et al. 2010) and be linked with the activation of  
33 352 transposable elements (Lorincz et al. 2004), together facilitating systemic responses to parasite  
34 353 infection (Wenzel and Piertney 2014).

1  
2  
3 354 Changes in DNA methylation were related to processes involved in responses to infection.  
4  
5 355 The first aspect of physiology that hosts have to shift during parasite infection is the immune  
6  
7 356 response. KEGG analysis for DMSs and DMRs (see SI Appendix II) identified modifications of  
8  
9 357 the Th1 and Th2 cell differentiation, the T cell receptor signaling pathways and the metabolic  
10  
11 358 pathways of purine and pyrimidine involved in cell proliferation (Li et al. 2011). All contribute to  
12  
13 359 the maintenance of immune functions and enhance disease tolerance and resistance in fish  
14  
15 360 (Seegmiller et al. 1977; Li and Gatlin 2006). Furthermore, we found a number of differentially  
16  
17 361 methylated genes that regulate immunity such as the *catenin delta 1* gene (*sp5l*) that is an important  
18  
19 362 component of the innate immune system involved in the signaling of macrophages (Yang et al.  
20  
21 363 2014). Similarly, we found differential methylation for i) the *integrin alpha 1* (*itga1*), part of the  
22  
23 364 inflammation response (Valdebenito et al. 2018) and the recruitment of leukocytes into damaged  
24  
25 365 tissues (Becker et al. 2013), ii) the *f-box protein 41* (*fbxo41*) involved in the regulation of innate  
26  
27 366 immunity and MHC recognition (Correa et al. 2013) as well as iii) the *neuropeptide FF receptor*  
28  
29 367 *2* (*npffr2b*) that is part of the regulation of mitogen-activated protein kinases (MAPKs). Some of  
30  
31 368 those genes were hypermethylated upon infection (e.g. *itga1*, *npffr2b*; supplementary table S4, SI  
32  
33 369 Appendix I). Since hypermethylation is commonly associated with gene repression (Artemov et  
34  
35 370 al. 2017), we likely captured elements of parasite manipulation that evolved to repress cell fate in  
36  
37 371 order to prevent cell turn over and the production of novel immune cells (Gómez-Díaz et al. 2012).

34 372 While MAPKs modulate cell responses, proliferation and apoptosis against pathogens  
35  
36 373 (Arthur and Ley 2013), recent studies in mice reported that MAPKs cascades such as ERK1-2 and  
37  
38 374 p38 play also a pivotal role in spermatogenesis, testis development and sperm motility (Almog and  
39  
40 375 Naor 2010). In our experiment, this could explain the differences in motile sperm concentration  
41  
42 376 observed (Kaufmann et al. 2014) between infected and uninfected sticklebacks. It is also known  
43  
44 377 that immune mechanisms, such as reactive oxygen species formation, alter sperm function further  
45  
46 378 linking infection to sperm traits (Guthrie and Welch 2012). Responding to parasite infection  
47  
48 379 necessitates the host to adjust metabolite production to support immune responses (Bize et al.  
49  
50 380 2010). These changes can either involve the elevation of the metabolism or the reallocation of  
51  
52 381 nutrients to fuel the costly defense mechanism (Bize et al. 2010; Rauw 2012). As such, differences  
53  
54 382 in the methylation status of genes involved in *fatty acid binding* or *protein citrate lyase* are likely  
55  
56 383 indirect effects of parasite exposure altering fish development and growth (Karasov and Martinez  
57  
58 384 Del Rio 2007). Noteworthy, a number of genes mediating methylation and transcription were

1  
2  
3 385 annotated, including *mepce* that is involved in RNA methylation and methyltransferase activity,  
4  
5 386 or *elmsan1b* that is related to chromatin binding (supplementary table S4, SI Appendix I). Overall,  
6  
7 387 these regulatory changes show that a natural parasite load in fish significantly impacts DNA  
8  
9 388 methylation cellular process mediating plastic response to cope with infection.

10 389 Contrary to differentially methylated sites and regions, individual genome-wide methylation  
11  
12 390 pattern showed fish family as the primary determinant of the distribution of DNA methylation.  
13  
14 391 This shows that the potential of genome-wide DNA methylation patterns is inheritable as it is not  
15  
16 392 independent of the nucleotide sequence (Dubin et al. 2015; Metzger and Schulte 2017; Rey et al.  
17  
18 393 2019). By extension, it implies that the adaptive potential of populations that includes DNA-  
19  
20 394 methylation is linked to the genetic diversity present in that population (Rey et al. 2019). Therefore,  
21  
22 395 it is likely that reduced genetic diversity within a population is also accompanied by reduced  
23  
24 396 methylation variation, and weaker responses to infection.

25 397 Overall, our study extends beyond the descriptive analyses of DNA methylation  
26  
27 398 modifications and gene ontology (Gugger et al. 2016; Artemov et al. 2017; Hu et al. 2018). By  
28  
29 399 controlling parasite load and fish genetic background, we gained new insights into the extent to  
30  
31 400 which parasite infection alters host's methylomes and suggests an important role of DNA  
32  
33 401 methylation in host-parasite interactions. We report the potential of methylation modifications,  
34  
35 402 which may serve as indicators of phenotypic shifts associated with parasite-mediated selection.  
36  
37 403 Future research should now focus on the role of DNA methylation in adaptive plasticity and its  
38  
39 404 relation to genetic diversity.  
40

405

## 406 **Materials and Methods**

### 407 **Sampling and infection experiments**

408 Three-spined sticklebacks (*Gasterosteus aculeatus*) were caught from a natural population in  
409 Northern Germany (Grosser Plöner See, 54°9'21.16" N, 10°25'50.14" E). By randomly pairing  
410 males and females, we obtained the first experimental parasite-free full-sib families (G1  
411 generation). Male juveniles of each G1 fish family were randomly assigned to one of two treatment  
412 groups: no parasite exposure (i.e., control) or exposed with *Camallanus lacustris*; a trophically  
413 transmitted nematode that infects the gut of sticklebacks and occurs naturally in the host population  
414 (Kalbe et al. 2009). The experiment was repeated twice independently in two consecutive years ( $N$   
415 = 28 and  $N = 24$ ). Using brother fish, we minimized the effects of genetic variation on DNA

1  
2  
3 416 methylation patterns, and hence any variation in DNA methylation changes across individuals can  
4  
5 417 be linked to treatment and family background. Including multiple families on the other hand allows  
6  
7 418 us to quantify the effects of the genetic background. In addition, to control for dosage effect and  
8  
9 419 eventually methylation levels, the number of larvae inside the intermediate host (a copepod) was  
10  
11 420 counted and each host was exposed twice to exactly six larvae of *C. lacustris*. For details on the  
12  
13 421 experimental design see Kaufmann et al. (2014). While the whole experiment consisted of ten  
14  
15 422 families, here we sequenced 52 males (25 infected and 27 uninfected fish brothers) belonging to  
16  
17 423 five families (supplementary table S1, SI Appendix I). For each fish, we counted the number of  
18  
19 424 parasites and measured (mean  $\pm$  std) a number of condition dependent traits such as organ weight  
20  
21 425 (liver, head-kidney and testes weight) and fish size. We also estimated the body condition as a  
22  
23 426 proxy fitness, using the residuals of the linear regression of log<sub>10</sub>-transformed weight against  
24  
25 427 log<sub>10</sub>-transformed body length. To obtain some estimates of the immune activation of the fish, we  
26  
27 428 measured the respiratory burst activity. Lastly, because the link between male treatment and the  
28  
29 429 next generation is shown in the sperm, we also measured elements of sperm motility and  
30  
31 430 concentration (Kaufmann et al. 2014) in some randomly assigned fish ( $N = 20$ ). Fitness traits of  
32  
33 431 samples have been analysed in Kaufmann et al. (2014).

### 32 432 **DNA extraction and Reduced-Representation Bisulfite Sequencing library preparation**

34 433 We used liver tissue to screen the DNA methylations of sticklebacks as a major metabolic regulator  
35  
36 434 and a lymphoid organ (Tarasenko and McGuire 2017). DNA extraction was performed with the  
37  
38 435 Qiagen DNeasy Blood and Tissue Kit (Qiagen, Hilden, Germany), according to the manufacturer's  
39  
40 436 protocol. Qubit™ fluorometric assay was used to assess the quality and quantity of DNA. DNA  
41  
42 437 methylated sites were identified by RRBS (Meissner et al. 2005) as done in Heckwolf and Meyer  
43  
44 438 et al. (unpublished data). For each fish, we constructed a single-end library of 100 bp that resulted  
45  
46 439 in an average of 11.5 million reads. Library preparation was carried out at the Institute for Clinical  
47  
48 440 Molecular Biology (IKMB; Germany) and sequencing took place on an Illumina HiSeq 2500  
49  
50 441 platform, with 18 individuals pooled per lane.

### 51 442 **Data processing and methylation calling**

52 443  
53 444 Raw sequence reads from the bisulfite-treated samples were analyzed with FASTQC v0.11.5  
54  
55 445 (Andrews 2010), processed and filtered to remove adaptor sequences and low-quality (i.e.,  $q$  lower  
56  
57  
58  
59  
60



1  
2  
3 447 than 20) reads with Cutadapt v1.13 (Martin 2011) using three adapter sequences  
4  
5 448 (NNAGATCGGAAGAGCACAC, AGATCGGAAGAGCACAC, ATCGGAAGAGCACAC).  
6  
7 449 We used Bismark v0.19.0 (Krueger and Andrews 2011) with the Bowtie2 v.2.3.2 aligner to align  
8  
9 450 reads to the three-spined stickleback reference genome (gasAcu1, Broad Institute) and to extract  
10  
11 451 methylated CpGs. Average mapping efficiency was  $67.3 \pm 3.0$  % (for summary of RRBS  
12  
13 452 sequencing see supplementary table S7, SI Appendix I). Output files from Bismark were further  
14  
15 453 processed in R version 3.4.1 (R Development Core Team 2015).

15 454 To analyze differential methylation, we used *MethylKit* R package v.1.5.0 (Akalin et al.  
16  
17 455 2012). Prior to DNA methylation analysis, we filtered CpG sites to process only those with  
18  
19 456 sufficient coverage ( $\geq 10X$ ). Sites that were in the 99.9<sup>th</sup> percentile of coverage were removed to  
20  
21 457 account for potential PCR bias. We kept only those methylated CpG sites observed in at least two  
22  
23 458 individual fish. To test for differentially methylated sites and differentially methylated regions  
24  
25 459 between treatments, we looked for sites that showed at least 15% differential fractional  
26  
27 460 methylation between infected and control fish and *q*-values lower than 0.01, using the SLIM  
28  
29 461 method. We then kept only those sites that were present in at least 50% of the fish within the  
30  
31 462 different treatment groups (infected and uninfected-control). To identify DMRs, we used the  
32  
33 463 *tileMethylCounts()* function in *MethylKit* v.1.5.0 with a sliding window size of 100 bases and step  
34  
35 464 size of 100 bases.

36 465

### 36 466 **Identification of single nucleotide polymorphisms**

37  
38 467 We used BISulfite-seq CUI Toolkit v0.2.2 (BISCUIT; <https://github.com/zwdzwd/biscuit>) to  
39  
40 468 identify single nucleotide polymorphisms across samples. Aligned RRBS reads were filtered  
41  
42 469 considering the following parameters: biallelic, minimum and maximum read coverage between  
43  
44 470  $5\times$  and  $100\times$ , minimum base quality of 20. We kept only those single nucleotide polymorphic sites  
45  
46 471 (SNPs) that were sequenced in all individuals. Variants were called and indels were filtered using  
47  
48 472 VCFtools v.0.1.5 (Danecek et al. 2011) with default settings. We then estimated the genetic  
49  
50 473 differentiation between and within families, using Wright's fixation index ( $F_{ST}$ ) as implemented  
51  
52 474 in VCFtools v.0.1.5 (Danecek et al. 2011).

53 475

### 53 476 **Statistical analyses**

1  
2  
3 477 All analyses were carried out in R version 3.4.1 (R Development Core Team 2015). Normality and  
4  
5 478 homoscedasticity of the data were investigated and whenever  $\log(x+1)$  transformation did not  
6  
7 479 match parametric assumptions, non-parametric tests were performed. First, we tested the effects  
8  
9 480 of parasite infection on fish fitness. We used LMM with family as a random effect and compared  
10  
11 481 the size of head kidney, liver, testes, body condition and motile sperm concentration between  
12  
13 482 infected and control fish, correcting for fish size when necessary.

14 483 For methylation analyses, we controlled for depth bias in DNA sequencing, using the ratio  
15  
16 484 of the number of methylated sites to the number of reads for all subsequent statistical analyses.  
17  
18 485 Number of methylated sites/regions were estimated by converting the methylation frequency into  
19  
20 486 ordinal data: sites/regions with little or no methylation ( $MFr < 30\%$ ) were annotated as 0 and  
21  
22 487 treated as no methylated sites/regions, sites/regions with intermediate methylation levels ( $30\% <$   
23  
24 488  $MFr < 70\%$ ) were considered as heterozygote sites/regions and converted into 1, whereas  
25  
26 489 sites/regions with high or fixed methylation ( $MFr > 70\%$ ) were treated as homozygous at this  
27  
28 490 site/regions and were annotated as 2. We used t-test for unequal variances to assess the difference  
29  
30 491 in RMS between infected and control fish. To account for genetic background, we also compared  
31  
32 492 RMS using LMM across treatments using family as a random effect. Similar tests were also  
33  
34 493 performed for RMR. As a next step, a series of LMM were performed fitting the interaction of  
35  
36 494 seven phenotypic traits (liver, head kidney and testes weights as well as body condition, respiratory  
37  
38 495 burst activity and motile sperm concentration) with treatment as fixed effects and methylation ratio  
39  
40 496 as dependent variable. To ensure that overall fish size was not a confounding factor, all measures  
41  
42 497 were corrected for fish length, while testes size was included as a covariate of motile sperm  
43  
44 498 concentration. Further details on LMM are available in SI Appendix SI Methods, Section SI.1.

41 499 To test for the consistency of DNA methylation modifications across individuals within a  
42  
43 500 treatment, we followed two approaches. We first conducted cluster analyses using the fractional  
44  
45 501 methylation data: i) PCA using the standard *prcomp()* function, ii) NMDS with Bray-Curtis  
46  
47 502 distance as well as iii) hierarchical clustering with 1000 bootstraps using Euclidean distance  
48  
49 503 method, with the *vegan* R package (Oksanen et al. 2013). We used the methylated CpG sites and  
50  
51 504 regions of each fish and explored how similar is the methylation pattern across individuals despite  
52  
53 505 different family backgrounds. Methylated sites and regions with low variation and a standard  
54  
55 506 deviation below 0.3, i.e. non-informative sites across individuals, were excluded from the cluster  
56  
57 507 analyses. To classify the number the specimens into clusters, we used the average silhouette

1  
2  
3 508 method with 100 bootstraps and set up the maximum number of  $k$ -means at 5 (equals the number  
4 of families), using the *factoextra* R package (Kassambara 2017). Alternatively, goodness of fit of  
5 509 NMDS and stress values were used to identify the best dimension for projection of NMDS based  
6 510 on Clarke (1993) guidelines using the *goeveg* R package (Goral and Schellenberg 2017). Second,  
7 511 we treated methylated sites as distinct separate loci and we estimated the pairwise  $F_{ST}$  and  $F_{IS}$   
8 512 values (i.e.,  $epi-F_{ST}$  and  $epi-F_{IS}$ , respectively) between individuals using the *genepop* R package  
9 513 (Rousset 2008). To do so, the methylation frequency of each CpG site was binary-encoded with  
10 514 the presence/absence of a methylation coded for as 1/0 as for AFLP datasets and converted to a  
11 515 diploid phase (SMP). Hence, non-methylated sites ( $MFr < 30\%$ ) were annotated as 0/0,  
12 516 heterozygote methylated sites ( $30\% < MFr < 70\%$ ) were converted into 0/1, whereas homozygote  
13 517 methylated sites ( $MFr > 70\%$ ) annotated as 1/1. We used linear mixed effect models, with family  
14 518 as a random effect to compare pairwise  $F_{ST}$  between exposed and control fish.  
15 519

16 520 For the DMS and DMR datasets we repeated the aforementioned cluster analyses.  
17 521 Additionally, we performed Maximum Parsimony phylogenetic analysis and constructed the  
18 522 relationships between individuals' methylation profiles. To do so, we treated the methylation ratio  
19 523 of each site as a multistate ordered character, ranged from 0 (no methylation) to 10 (methylated  
20 524 site). We then conducted the Shimodaira-Hasegawa test (Shimodaira and Hasegawa 1999) with  
21 525 RELL bootstrap with 1000 replicates in PAUP v.4.0b10 (Swofford 2002). We constructed two  
22 526 trees: one matching the different families and another one matching perfectly the two treatment  
23 527 groups and tested the hypothesis that DMS and DMR patterns are more closely related to treatment  
24 528 specific than to family specific clustering. Our findings for DMRs is given in Supporting  
25 529 Information (SI) Appendix II.  
26 530

27 531

### 28 532 **Functional annotation and pathways analyses**

29 533 For the functional annotation, we used the ENSEMBL stickleback database (release 90) and the  
30 534 *genomation* R package v.1.1.0 (Akalın et al. 2015). We identified the genomic feature (i.e., exon,  
31 535 intron, promoter and intergenic region) of each methylated CpG, DMSs and DMRs, giving  
32 536 precedence to the following order promoters, exons, introns and intergenic regions when features  
33 537 overlapped (Akalın et al. 2015). We define promoter region as 1500 bp upstream and 500 bp  
34 538 downstream from the transcription starting site (TSS). Chi-square test was used to examine  
35 539 whether DMSs or DMRs were randomly distributed or not within the different genomic features.  
36 540  
37 541  
38 542  
39 543  
40 544  
41 545  
42 546  
43 547  
44 548  
45 549  
46 550  
47 551  
48 552  
49 553  
50 554  
51 555  
52 556  
53 557  
54 558  
55 559  
56 560  
57 561  
58 562  
59 563  
60 564

1  
2  
3 539 Furthermore, we run chi-square test to evaluate how methylated CpGs are distributed in infected  
4 540 compared to control fish. To consider a gene to be differentially methylated, methylated CpGs,  
5 541 DMSs and DMRs had to be located no further than 1.5 kilobase upstream and 500 bases  
6 542 downstream of it. To find the nearest TSS to a differentially methylated site or region, we used the  
7 543 *GenomicRanges* R package v.1.30.0 (Lawrence et al. 2013).

8 544 Differentially methylated genes were further used for GO enrichment analysis. Significant  
9 545 over- or under-representation of GO terms was obtained using the *GOstats* R package v.2.44.0  
10 546 (Falcon and Gentleman 2007). Gene functions were categorized based on biological process,  
11 547 molecular function and cellular component. *P*-values were corrected for multiple testing using a  
12 548 false discovery rate. In addition, we conducted a pathway analysis, using the KEGG enrichment  
13 549 analysis implemented in BLAST2GO version 4.1 (Conesa et al. 2005) to identify functional  
14 550 associations among differentially methylated genes. Functional enrichment analyses for DMRs are  
15 551 given in SI Appendix II. Finally, to ensure the adaptive value of differential methylation we tested  
16 552 whether lower methylated genes among parasite treated samples predict greater fitness running  
17 553 correlation tests.

18 554

### 19 555 **Acknowledgements**

20 556 The work presented in this manuscript was supported by a Marie Curie Intra-European Fellowship  
21 557 Program to K.S. (project 'TGIP', 704673) as well as German Science Foundation grants (DFG,  
22 558 EI841/4-1 and EI 841/6-1) to C.E. The authors thank G. Augustin and D. Martens for their help  
23 559 maintaining the fish, M. Schwartz and R. Leipnitz for their help in the copepod work and N.  
24 560 Wildenhayn, W. Derner, G. Schmiedeskamp and Henrike Schmidt for their help in laboratory  
25 561 procedure. We would also like to thank two anonymous reviewers for their constructive and  
26 562 insightful comments on previous versions of this manuscript.

27 563

### 28 564 **Author Contributions**

29 565 K.S. and C.E. conceived and designed the study with substantial contributions for the bisulfite  
30 566 sequencing strategy from B.S.M.. T.L.L. and C.E. helped design the breeding experiments. J.K.  
31 567 carried out the breeding experiment as well as the infection experiment and measured fitness traits.  
32 568 K.S. conducted wet lab work (DNA extraction). K.S. and B.S.M. analyzed the data for which  
33 569 B.S.M. provided key scripts. C.E. advised the analyses. K.S. and CE drafted the manuscript. R.H.

1  
2  
3 570 conducted the library preparation and sequencing. All co-authors contributed to the final version  
4 of the manuscript.  
5 571  
6  
7 572

### 8 573 **Supplementary Material**

9  
10 574 **Supplementary Information Appendix I:** Methodological details, supplementary results, figures  
11 and tables are provided in Appendix I.  
12 575

13 576 **Supplementary Information Appendix II:** Results of differentially methylated regions (DMRs)  
14 are provided in Appendix II.  
15 577  
16  
17 578

18  
19 579 **Data Access:** The data generated in this study will be available upon publication  
20  
21 580

### 22 581 **References**

- 23  
24 582 Akalin A, Franke V, Vlahoviček K, Mason CE, Schübeler D. 2015. Genomation: a toolkit to  
25 summarize, annotate and visualize genomic intervals. *Bioinformatics*. 31(7): 1127-1129.  
26 583  
27 584 Akalin A, Kormaksson M, Li S, Garrett-Bakelman FE, Figueroa ME, Melnick A, Mason CE.  
28 2012. methylKit: a comprehensive R package for the analysis of genome-wide DNA  
29 585 methylation profiles. *Genome Biol*. 13(10): R87.  
30 586  
31 587 Alavioon G, Hotzy C, Nakhro K, Rudolf S, Scofield DG, Zajitschek S, Maklakov AA, Immler S.  
32 2017. Haploid selection within a single ejaculate increases offspring fitness. *Proc Natl*  
33 588 *Acad Sci USA*. 114(30): 8053-8058.  
34 589  
35 590 Almog T, Naor Z. 2010. The role of mitogen activated protein kinase (MAPK) in sperm  
36 591 functions. *Mol Cell Endocrinol*. 314(2): 239-243.  
37 592  
38 592 Altizer S, Harvell D, Friedle E. 2003. Rapid evolutionary dynamics and disease threats to  
39 593 biodiversity. *Trends Ecol Evol*. 18(11): 589-596.  
40 594  
41 594 Andrews S. 2010. FastQC: a quality control tool for high throughput sequence data. Available  
42 595 online at: <http://www.bioinformatics.babraham.ac.uk/projects/fastqc>.  
43 596  
44 596 Artemov AV, Muge NS, Rastorguev SM, Zhenilo S, Mazur AM, Tsygankova SV, Boulygina  
45 597 ES, Kaplun D, Nedoluzhko AV, Medvedeva YA, et al. 2017. Genome-wide DNA  
46 598 methylation profiling reveals epigenetic adaptation of stickleback to marine and  
47 599 freshwater conditions. *Mol Biol Evol*. 34(9): 2203-2213.  
48  
49  
50  
51  
52  
53  
54  
55  
56  
57  
58  
59  
60

- 1  
2  
3 600 Arthur JSC, Ley SC. 2013. Mitogen-activated protein kinases in innate immunity. *Nat Rev*  
4 601 *Immunol.* 13679.
- 6 602 Becker HM, Rullo J, Chen M, Ghazarian M, Bak S, Xiao H, Hay JB, Cybulsky MI. 2013.  $\alpha 1\beta 1$   
8 603 Integrin-mediated adhesion inhibits macrophage exit from a peripheral inflammatory  
9 604 lesion. *J Immunol.* 190(8): 4305-4314.
- 11 605 Beemelmans A, Roth O. 2017. Grandparental immune priming in the pipefish *Syngnathus*  
13 606 *typhle*. *BMC Evol Biol.* 17(1): 44.
- 15 607 Bérénos C, Wegner KM, Schmid-Hempel P. 2011. Antagonistic coevolution with parasites  
16 608 maintains host genetic diversity: an experimental test. *Proc R Soc B Biol Sci.* 278(1703):  
18 609 218-224.
- 20 610 Bird AP. 1984. Gene expression: DNA methylation - how important in gene control? *Nature.*  
21 611 307503.
- 24 612 Bize P, Piault R, Gasparini J, Roulin A. 2010. Indirect costs of parasitism are shaped by variation  
25 613 in the type of immune challenge and food availability. *Evol Biol.* 37(4): 169-176.
- 27 614 Brunner FS, Anaya-Rojas JM, Matthews B, Eizaguirre C. 2017. Experimental evidence that  
28 615 parasites drive eco-evolutionary feedbacks. *Proc Natl Acad Sci USA.* 114(14): 3678-  
29 616 3683.
- 32 617 Brunner FS, Eizaguirre C. 2016. Can environmental change affect host/parasite-mediated  
33 618 speciation? *Zoology.* 119(4): 384-394.
- 36 619 Clarke KR. 1993. Non-parametric multivariate analyses of changes in community structure. *Aust*  
37 620 *J Ecol.* 18(1): 117-143.
- 39 621 Conesa A, Götz S, García-Gómez JM, Terol J, Talón M, Robles M. 2005. Blast2GO: a universal  
40 622 tool for annotation, visualization and analysis in functional genomics research.  
41 623 *Bioinformatics.* 21(18): 3674-3676.
- 44 624 Correa RL, Bruckner FP, de Souza Cascardo R, Alfenas-Zerbini P. 2013. The role of f-box  
45 625 proteins during viral infection. *Int J Mol Sci.* 14(2): 4030-4049.
- 48 626 Danecek P, Auton A, Abecasis G, Albers CA, Banks E, DePristo MA, Handsaker RE, Lunter G,  
49 627 Marth GT, Sherry ST, et al. 2011. The variant call format and VCFtools. *Bioinformatics.*  
50 628 27(15): 2156-2158.
- 53  
54  
55  
56  
57  
58  
59

- 1  
2  
3 629 Downen RH, Pelizzola M, Schmitz RJ, Lister R, Downen JM, Nery JR, Dixon JE, Ecker JR. 2012.  
4  
5 630 Widespread dynamic DNA methylation in response to biotic stress. *Proc Natl Acad Sci*  
6  
7 631 *USA*. 109(32): E2183-E2191.
- 8  
9 632 Dubin MJ, Zhang P, Meng D, Remigereau M-S, Osborne EJ, Paolo Casale F, Drewe P, Kahles  
10  
11 633 A, Jean G, Vilhjálmsson B, et al. 2015. DNA methylation in *Arabidopsis* has a genetic  
12  
13 634 basis and shows evidence of local adaptation. *eLife*. 4e05255.
- 14  
15 635 Eizaguirre C, Baltazar-Soares M. 2014. Evolutionary conservation - evaluating the adaptive  
16  
17 636 potential of species. *Evol Appl*. 7(9): 963-967.
- 18  
19 637 Eizaguirre C, Lenz TL, Kalbe M, Milinski M. 2012. Rapid and adaptive evolution of MHC genes  
20  
21 638 under parasite selection in experimental vertebrate populations. *Nat Comm*. 3621-626.
- 22  
23 639 Eizaguirre C, Yeates SE, Lenz TL, Kalbe M, Milinski M. 2009. MHC-based mate choice  
24  
25 640 combines good genes and maintenance of MHC polymorphism. *Mol Ecol*. 18(15): 3316-  
26  
27 641 3329.
- 28  
29 642 Falcon S, Gentleman R. 2007. Using GOstats to test gene lists for GO term association.  
30  
31 643 *Bioinformatics*. 23(2): 257-258.
- 32  
33 644 Frankham R, Ballou JD, Briscoe DA. 2002. Introduction to conservation genetics. Cambridge,  
34  
35 645 UK: Cambridge University Press.
- 36  
37 646 Gómez-Díaz E, Jordà M, Peinado MA, Rivero A. 2012. Epigenetics of host-pathogen  
38  
39 647 interactions: the road ahead and the road behind. *PLoS Pathog*. 8(11): e1003007.
- 40  
41 648 Goral F, Schellenberg J. 2017. goeveg: Functions for community data and ordinations. R  
42  
43 649 package version 0.3.3.
- 44  
45 650 Gugger PF, Fitz-Gibbon S, PellEgrini M, Sork VL. 2016. Species-wide patterns of DNA  
46  
47 651 methylation variation in *Quercus lobata* and their association with climate gradients. *Mol*  
48  
49 652 *Ecol*. 25(8): 1665-1680.
- 50  
51 653 Guthrie HD, Welch GR. 2012. Effects of reactive oxygen species on sperm function.  
52  
53 654 *Theriogenology*. 78(8): 1700-1708.
- 54  
55 655 Heckwolf MJ, Meyer BS, Häsler R, Höppner MP, Eizaguirre C, Reusch TBH. 2019. Two  
56  
57 656 different epigenetic pathways detected in wild three-spined sticklebacks are involved in  
58  
59 657 salinity adaptation. *bioRxiv*649574.
- 60

- 1  
2  
3 658 Hu J, Pérez-Jvostov F, Blondel L, Barrett RDH. 2018. Genome-wide DNA methylation  
4 659 signatures of infection status in Trinidadian guppies (*Poecilia reticulata*). *Mol Ecol*.  
5 660 27(15): 3087-3102.
- 6  
7  
8 661 Kalbe M, Eizaguirre C, Dankert I, Reusch TBH, Sommerfeld RD, Wegner KM, Milinski M.  
9 662 2009. Lifetime reproductive success is maximized with optimal major histocompatibility  
10 663 complex diversity. *Proc R Soc Lond B*. 276(1658): 925-934.
- 11  
12  
13 664 Karasov WH, Martinez Del Rio C. 2007. Physiological ecology: How animals process energy,  
14 665 nutrients, and toxins. New Jersey, US: Princeton University Press.
- 15  
16  
17 666 Kassambara A. 2017. factoextra: Extract and visualize the results of multivariate data analyses. R  
18 667 package version 1.0.5.
- 19  
20  
21 668 Kaufmann J, Lenz TL, Milinski M, Eizaguirre C. 2014. Experimental parasite infection reveals  
22 669 costs and benefits of paternal effects. *Ecol Lett*. 17(11): 1409-1417.
- 23  
24 670 Kawakatsu T, Huang S-sC, Jupe F, Sasaki E, Schmitz RJ, Urich MA, Castanon R, Nery JR,  
25 671 Barragan C, He Y, et al. 2016. Epigenomic diversity in a global collection of *Arabidopsis*  
26 672 *thaliana* accessions. *Cell*. 166(2): 492-505.
- 27  
28  
29 673 Kekäläinen J, Soler C, Veentaus S, Huuskonen H. 2015. Male investments in high quality sperm  
30 674 improve fertilization success, but may have negative impact on offspring fitness in  
31 675 whitefish. *PLOS ONE*. 10(9): e0137005.
- 32  
33  
34 676 Kronholm I, Bassett A, Baulcombe D, Collins S. 2017. Epigenetic and Genetic Contributions to  
35 677 Adaptation in *Chlamydomonas*. *Mol Biol Evol*. 34(9): 2285-2306.
- 36  
37  
38 678 Krueger F, Andrews SR. 2011. Bismark: a flexible aligner and methylation caller for Bisulfite-  
39 679 Seq applications. *Bioinformatics*. 27(11): 1571-1572.
- 40  
41  
42 680 Kurtz J, Wegner KM, Kalbe M, Reusch TBH, Schaschl H, Hasselquist D, Milinski M. 2006.  
43 681 MHC genes and oxidative stress in sticklebacks: an immuno-ecological approach. *Proc R*  
44 682 *Soc Lond B*. 273(1592): 1407-1414.
- 45  
46  
47 683 Lawrence M, Huber W, Pagès H, Aboyoun P, Carlson M, Gentleman R, Morgan MT, Carey VJ.  
48 684 2013. Software for computing and annotating genomic ranges. *PLoS Comput Biol*. 9(8):  
49 685 e1003118.
- 50  
51  
52 686 Lenz TL, Eizaguirre C, Rotter B, Kalbe M, Milinski M. 2013. Exploring local immunological  
53 687 adaptation of two stickleback ecotypes by experimental infection and transcriptome-wide  
54 688 digital gene expression analysis. *Mol Ecol*. 22(3): 774-786.



- 1  
2  
3 689 Lev Maor G, Yearim A, Ast G. 2015. The alternative role of DNA methylation in splicing  
4 regulation. *Trends Genet.* 31(5): 274-280.  
5 690  
6 691 Li P, Gatlin DM. 2006. Nucleotide nutrition in fish: Current knowledge and future applications.  
7 *Aquaculture.* 251(2): 141-152.  
8 692  
9 693 Li Z, Zhang Y, Sun B. 2011. Current understanding of Th2 cell differentiation and function.  
10 *Protein Cell.* 2(8): 604-611.  
11 694  
12 695 Liu S, Sun K, Jiang T, Feng J. 2015. Natural epigenetic variation in bats and its role in evolution.  
13 *J Exp Biol.* 218(1): 100-106.  
14 696  
15 697 Lorincz MC, Dickerson DR, Schmitt M, Groudine M. 2004. Intragenic DNA methylation alters  
16 chromatin structure and elongation efficiency in mammalian cells. *Nat Struct Mol Biol.*  
17 698 111068.  
18 699  
19 700 Marr AK, MacIsaac JL, Jiang R, Airo AM, Kobor MS, McMaster WR. 2014. *Leishmania*  
20 *donovani* infection causes distinct epigenetic DNA methylation changes in host  
21 macrophages. *PLoS Pathog.* 10(10): e1004419.  
22 701  
23 702 Martin M. 2011. Cutadapt removes adapter sequences from high-throughput sequencing reads.  
24 *EMBnet.journal.* 17(1): 10-12.  
25 703  
26 704 Maunakea AK, Nagarajan RP, Bilenky M, Ballinger TJ, D'Souza C, Fouse SD, Johnson BE,  
27 Hong C, Nielsen C, Zhao Y, et al. 2010. Conserved role of intragenic DNA methylation  
28 in regulating alternative promoters. *Nature.* 466253.  
29 705  
30 706 Meissner A, Gnirke A, Bell GW, Ramsahoye B, Lander ES, Jaenisch R. 2005. Reduced  
31 representation bisulfite sequencing for comparative high-resolution DNA methylation  
32 analysis. *Nucleic Acids Res.* 33(18): 5868-5877.  
33 707  
34 708 Merilä J, Hendry AP. 2014. Climate change, adaptation, and phenotypic plasticity: the problem  
35 and the evidence. *Evol Appl.* 7(1): 1-14.  
36 709  
37 710 Metzger DCH, Schulte PM. 2017. Persistent and plastic effects of temperature on DNA  
38 methylation across the genome of threespine stickleback (*Gasterosteus aculeatus*). *Proc*  
39 *R Soc B Biol Sci.* 284(1864).  
40 711  
41 712 Morandini AC, Santos CF, Yilmaz Ö. 2016. Role of epigenetics in modulation of immune  
42 response at the junction of host–pathogen interaction and danger molecule signaling.  
43 *Pathog Dis.* 74(7): ftw082.  
44 713  
45 714  
46 715  
47 716  
48 717  
49 718

- 1  
2  
3 719 Oksanen J, Blanchet FG, Kindt R, Legendre P, Minchin PR, O'Hara RB, Simpson GL, Solymos  
4 P, Stevens MHH, Wagne H. 2013. Vegan: community ecology package. R package  
5 720  
6 721 version 2.0-3.
- 7  
8 722 Potok ME, Nix DA, Parnell TJ, Cairns BR. 2013. Reprogramming the Maternal Zebrafish  
9 723  
10 724 Genome after Fertilization to Match the Paternal Methylation Pattern. *Cell*. 153(4): 759-  
11 772.
- 12  
13 725 R Development Core Team. 2015. R: a language and environment for statistical computing.  
14 726  
15 727 Vienna, Austria: R Foundation for Statistical Computing.
- 16  
17 728 Rauw WM. 2012. Immune response from a resource allocation perspective. *Front Genet*. 3267.  
18  
19 729 Rey O, Eizaguirre C, Angers B, Baltazar-Soares M, Sagonas K, Prunier JG, Blanchet S. 2019.  
20 730  
21 731 Linking epigenetics and biological conservation: Towards a conservation epigenetics  
22 732  
23 733 perspective. *Functional Ecology*. 001-14.
- 24 734 Riggs AD, Xiong Z, Wang L, LeBon JM. 2007. Methylation dynamics, epigenetic fidelity and X  
25 735  
26 736 chromosome structure. In: Chadwick DJ, G. C, editors. *Novartis Foundation Symposium*  
27 214 - Epigenetics. Chichester, UK: John Wiley & Sons, Ltd.
- 28  
29 737 Robertson M, Schrey A, Shayter A, Moss CJ, Richards C. 2017. Genetic and epigenetic variation  
30 738  
31 739 in *Spartina alterniflora* following the Deepwater Horizon oil spill. *Evol Appl*. 10792-  
32 801.
- 33  
34 740 Rousset F. 2008. Genepop'007: a complete reimplementation of the Genepop software for  
35 741  
36 742 Windows and Linux. *Mol Ecol Resour*. 8103-106.
- 37  
38 743 Seegmiller JE, Watanabe T, Shreier MH, Waldmann TA. 1977. Immunological aspects of purine  
39 744  
40 745 metabolism. *Adv Exp Med Biol*. 76A412-433.
- 41  
42 746 Seisenberger S, Peat JR, Hore TA, Santos F, Dean W, Reik W. 2013. Reprogramming DNA  
43 747  
44 748 methylation in the mammalian life cycle: building and breaking epigenetic barriers. *Phil*  
45  
46 749 *Trans R Soc B*. 368(1609): 20110330-20110330.
- 47  
48 750 Sheldon EL, Schrey A, Andrew SC, Ragsdale A, Griffith SC. 2018. Epigenetic and genetic  
49 751  
50 752 variation among three separate introductions of the house sparrow (*Passer domesticus*)  
51 753  
52 754 into Australia. *R Soc Open Sci*. 5(4): 172185.
- 53  
54 755 Shimodaira H, Hasegawa M. 1999. Multiple comparisons of log-likelihoods with applications to  
55 756  
56 757 phylogenetic inference. *Mol Biol Evol*. 16(8): 1114-1116.
- 57  
58  
59  
60

- 1  
2  
3 749 Skvortsova K, Iovino N, Bogdanović O. 2018. Functions and mechanisms of epigenetic  
4 inheritance in animals. *Nat Rev Mol Cell Biol.* 19(12): 774-790.  
5 750  
6  
7 751 Smith G, Smith C, Kenny JG, Chaudhuri RR, Ritchie MG. 2015. Genome-wide DNA  
8 752 methylation patterns in wild samples of two morphotypes of threespine stickleback  
9 (*Gasterosteus aculeatus*). *Mol Biol Evol.* 32(4): 888-895.  
10 753  
11  
12 754 Smith TA, Martin MD, Nguyen M, Mendelson TC. 2016. Epigenetic divergence as a potential  
13 first step in darter speciation. *Mol Ecol.* 25(8): 1883-1894.  
14 755  
15 756 Swofford DL. 2002. PAUP\*. Phylogenetic analysis using parsimony (\*and other methods).  
16 Massachusetts, USA: Sinauer Associates, Sunderland, MA.  
17 757  
18  
19 758 Tarasenko TN, McGuire PJ. 2017. The liver is a metabolic and immunologic organ: A  
20 reconsideration of metabolic decompensation due to infection in inborn errors of  
21 759 metabolism (IEM). *Mol Genet Metab.* 121(4): 283-288.  
22 760  
23  
24 761 Thorson JLM, Smithson M, Beck D, Sadler-Riggelman I, Nilsson E, Dybdahl M, Skinner MK.  
25 2017. Epigenetics and adaptive phenotypic variation between habitats in an asexual snail.  
26 762 *Sci Rep.* 7(1): 14139.  
27 763  
28  
29 764 Valdebenito S, Barreto A, Eugenin EA. 2018. The role of connexin and pannexin containing  
30 channels in the innate and acquired immune response. *Biochimica et Biophysica Acta*  
31 765 (BBA) - Biomembranes. 1860(1): 154-165.  
32 766  
33  
34 767 Wenzel MA, Piertney SB. 2014. Fine-scale population epigenetic structure in relation to  
35 gastrointestinal parasite load in red grouse (*Lagopus lagopus scotica*). *Mol Ecol.* 23(17):  
36 768 4256-4273.  
37 769  
38  
39 770 West-Eberhard MJ. 2003. *Developmental Plasticity and Evolution*. Oxford: Oxford University  
40 Press.  
41 771  
42  
43 772 Yang Z, Sun D, Yan Z, Reynolds AB, Christman JW, Minshall RD, Malik AB, Zhang Y, Hu G.  
44 2014. Differential Role for p120-Catenin in Regulation of TLR4 Signaling in  
45 773 Macrophages. *J Immunol.* 193(4): 1931-1941.  
46 774  
47  
48  
49 775  
50  
51 776  
52  
53  
54  
55  
56  
57  
58  
59  
60

## 777 **Figure Legends**

778 **Fig. 1.** Parasite infection induces changes in DNA methylation levels. We represent the ratio of  
779 methylated sites (RMS). The overall fractional methylation is also given for each treatment group.  
780 Error bars represent  $\pm 1$  SD.

781 **Fig. 2.** Cluster analyses of individual fish methylomes. A) Non-metric dimensional scaling  
782 (NMDS) and B) Principal component analysis (PCA). Goodness of fit for NMDS suggested the  
783 presence of five dimensions with a stress value lower than 0.1. Families are distinguished by  
784 different colors. Squares indicate control fish and crosses indicate parasite exposed and infected  
785 fish. Ellipses in PCA graph denote the 95% confidence intervals. C) Hierarchical clustering. *K*-  
786 mean indicated the presence of three major clades. Within each clade families are separated from  
787 one another. Light grey refers to control and dark grey to infected.

788 **Fig. 3.** Differentially methylated sites. A) Manhattan plot of the differentially methylated CpG  
789 sites (DMS) across chromosomes between infected and uninfected fish. The y axis represents the  
790 methylation percentage of the difference for a position. Only DMS higher than 15% change in  
791 methylation are presented. B) Barplot of the number of hypermethylated sites per chromosome  
792 between infected and control fish. C) Number of DMS and their associated genes of the  
793 randomized sets. Black vertical line indicates the average number of DMS and genes of the  
794 randomized sets, while the grey line refers to the number of DMS and genes of the original dataset.

795 **Fig. 4.** Cluster analyses for differentially methylated sites between treatments. A) PCA for the  
796 differentially methylated sites between infected and control fish brothers. Principal component 2  
797 axis (15.5%) separates fish based on their treatment. Squares denote fish exposed to parasites and  
798 crosses denote the control ones. Families are highlighted with different colors. Ellipses represent  
799 the 95% confident intervals. B) *k*-mean statistics for differentially methylated sites suggested the  
800 presence of two groups that match the infection treatments (Shimodaira-Hasegawa test). C)  
801 Hierarchical clustering. *K*-mean indicated the presence of two major clades that fit better with  
802 treatment specific rather than family. Treatment bar: open grey refers to control and dark grey to  
803 infected.

804 **Fig. 5.** Gene ontology terms. Biological processes and molecular functions that are  
805 hypermethylated in control and infected fish, as well as GO terms for differentially methylated  
806 sites between the two groups. The size of the circle refers to the number of genes observed in the

1  
2  
3 807 group that are associated with this term, and the shading of the circle to the *P*-value (darker circles  
4  
5 808 refer to a lower *P*-value). DM refers to differentially methylated genes.  
6  
7  
8  
9  
10  
11  
12  
13  
14  
15  
16  
17  
18  
19  
20  
21  
22  
23  
24  
25  
26  
27  
28  
29  
30  
31  
32  
33  
34  
35  
36  
37  
38  
39  
40  
41  
42  
43  
44  
45  
46  
47  
48  
49  
50  
51  
52  
53  
54  
55  
56  
57  
58  
59  
60

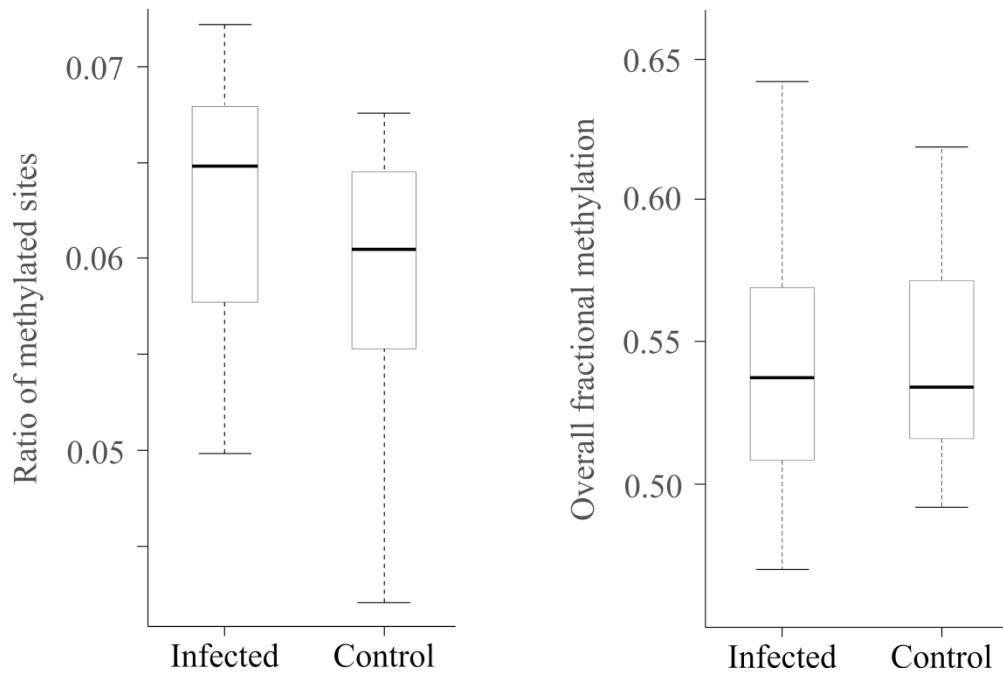


Fig. 1. Parasite infection induces changes in DNA methylation levels. We represent the ratio of methylated sites (RMS). Furthermore, the overall fractional methylation is given for each treatment group. Error bars represent  $\pm 1$  SD.

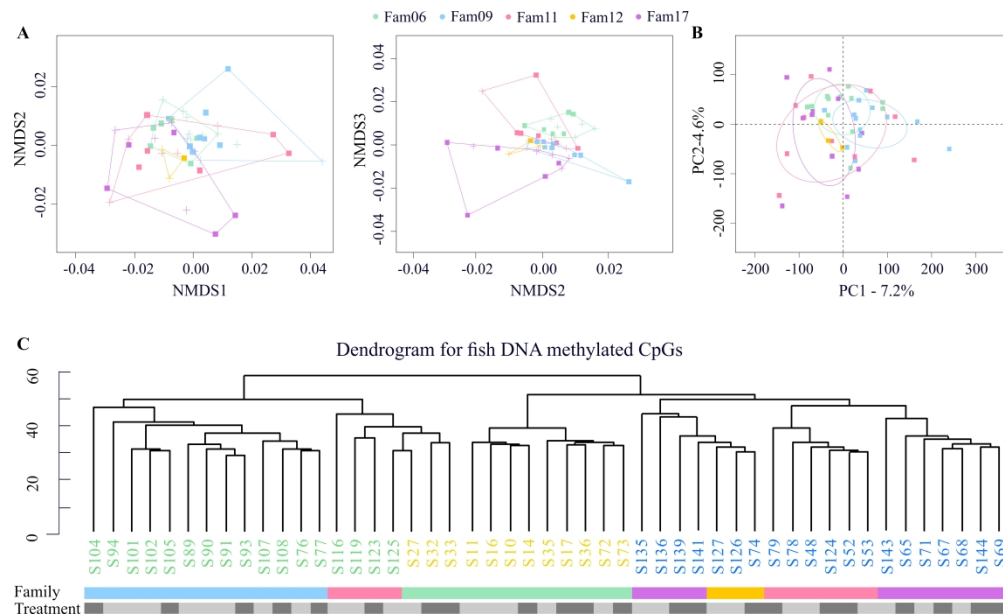


Fig. 2. Cluster analyses of individual fish methylomes. A) Non-metric dimensional scaling (NMDS) and B) Principal component analysis (PCA). Goodness of fit for NMDS suggested the presence of five dimensions with a stress value lower than 0.1. Families are distinguished by different colors. Squares indicate control fish and crosses indicate parasite exposed and infected fish. Ellipses in PCA graph denote the 95% confidence intervals. C) Hierarchical clustering. K-mean indicated the presence of three major clades. Within each clade the families are well distinguished from one another. Treatment bar: light grey refers to control and dark grey to infected.

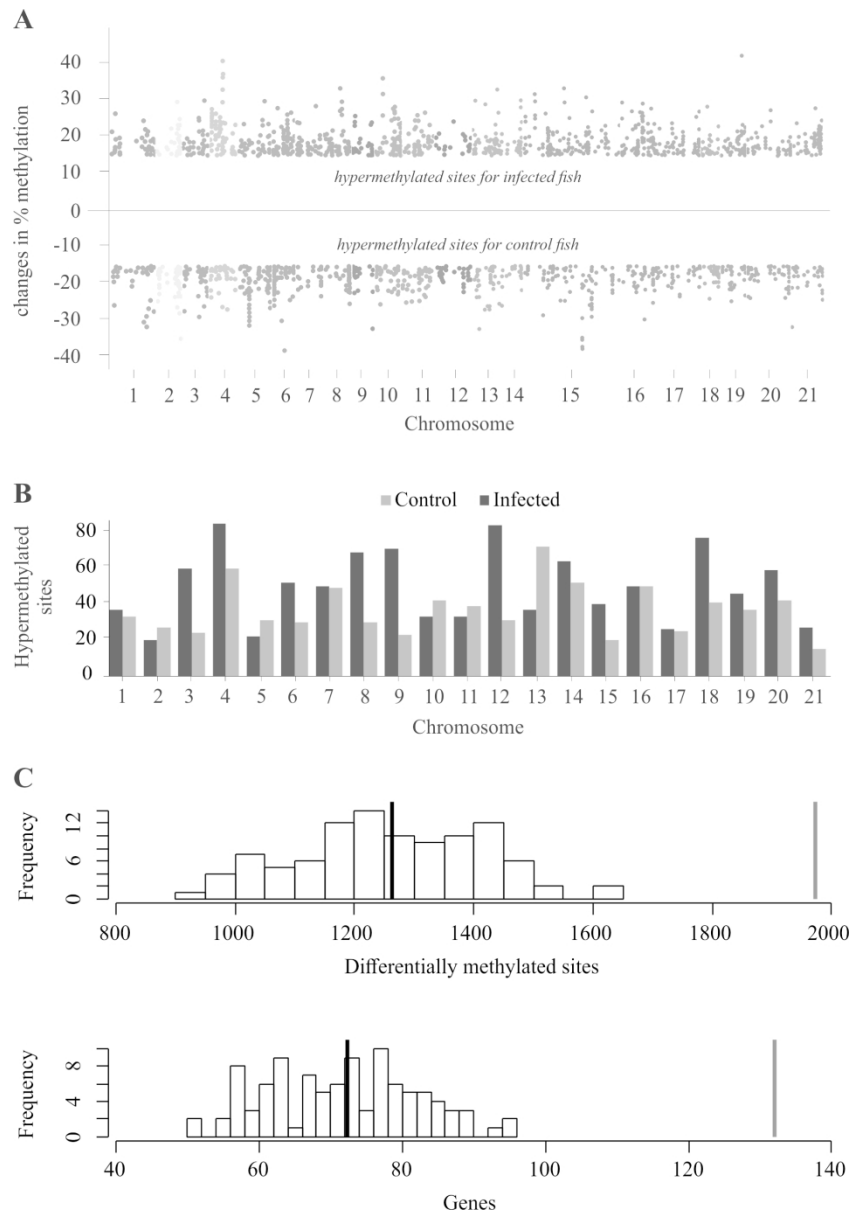


Fig. 3. Differentially methylated sites. A) Manhattan plot of the differentially methylated CpG sites (DMS) across chromosomes between infected and uninfected fish. The y axis represents the methylation percentage of the difference for a position. Only DMS higher than 15% change in methylation are presented. B) Barplot of the number of hypermethylated sites per chromosome between infected and control fish. C) Number of DMS and their associated genes of the randomized sets. Black vertical line indicates the average number of DMS and genes of the randomized sets, while the grey line refers to the number of DMS and genes of the original dataset.

161x231mm (300 x 300 DPI)



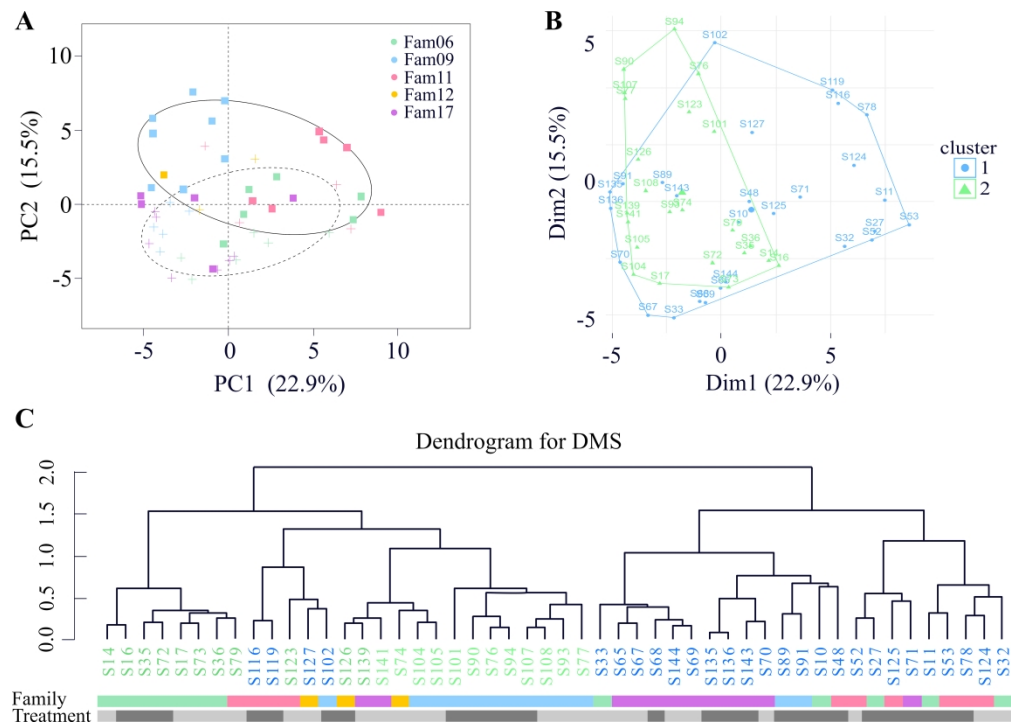


Fig. 4. Cluster analyses for differentially methylated sites between treatments. A) PCA for the differentially methylated sites between infected and control fish brothers. Principal component 2 axis (15.5%) separates fish based on their treatment. Squares denote exposed to parasite fish and crosses denote the control ones. Families are highlighted with different colors. Ellipses represent the 95% confident intervals. B) k-mean statistics for differentially methylated sites suggested the presence of two groups that match the infection treatments (Shimodaira-Hasegawa test). C) Hierarchical clustering. K-mean indicated the presence of two major clades that fit better with treatment specific rather than family. Treatment bar: open grey refers to control and dark grey to infected.

1  
2  
3  
4  
5  
6  
7  
8  
9  
10  
11  
12  
13  
14  
15  
16  
17  
18  
19  
20  
21  
22  
23  
24  
25  
26  
27  
28  
29  
30  
31  
32  
33  
34  
35  
36  
37  
38  
39  
40  
41  
42  
43  
44  
45  
46  
47  
48  
49  
50  
51  
52  
53  
54  
55  
56  
57  
58  
59  
60



Fig. 5. Gene ontology terms. Biological processes and molecular functions that are hypermethylated in control and infected fish, as well as GO terms for differentially methylated sites between the two groups. The size of the circle refers to the number of genes observed in the group that are associated with this term, and the shading of the circle to the P-value (darker circles refer to a lower P-value). DM refers to differentially methylated genes.

148x240mm (300 x 300 DPI)